REMARKS

Claims 51 - 72 remain active in the case. Claim 73 has been cancelled as redundant in view of amended claim 51.

Serum-free culture medium is supported on page 26, lines 4 – 6 ("The neurons are grown...in serum-free media. The cells are cultured in defined media...") and on page 30, lines 17 – 20 (The NG-108-15 cell line,... has been shown to provide reproducible results. Most of the data has been collected with this cell type and they have been shown to live two or three months in our defined culture system. The lifespan of the primary CNS cells in our defined or reproducible cell culture system is about a month.")

The added limitation reciting an intervening layer acting as a high-impedance seal is supported in the specification at page 11, lines 6 – 12.

Deconvoluting changes to identify one or more ion channels affected by the test substance is supported on page 7, lines 13 – 28 and page 10, lines 4 – 16.

The amendments are supported fully by the claims and/or specification as originally filed and, thus, do not represent new subject matter.

With regard to serum-free media, all of the initial work on neuronal cell cultures was done in what was called "serum-containing media." This was generally bovine serum and was though to be essential for culture of neuronal and cardiac cell cultures. However, the serum was found to vary between cows, as well as the day and even the time of day that it was drawn. In the late 80's and early 90's a small number of groups started exploring the idea of having a defined or "serum-free" media composition for primary neuronal culture as well as neuronal cell lines. This serum-free formulation has many advantages over serum-containing media in the present invention because the proteins in serum interfere with the intervening layer and prevent one from obtaining a sufficiently sensitive system to perform the deconvolution analysis.

In 1995, in collaboration with the National Institute of Health, we published the first paper that extended the idea of a defined growth media to include a synthetic chemical surface and neuronal cell culture preparation procedure to create the first defined system for neuronal cell culture. (Schaffner et al., submitted herewith).

The concept of deconvolution of an action potential, or any signal for that matter, implies that some prior knowledge of the factors contributing to the shapes are known. It is well known that an action potential requires the contributions of ion fluxes through at least three distinct ion channels. Varying the contributions of these ion fluxes from these channels has been shown to very the shape of the action potential, and this is illustrated in Figures 5 and 6A. of the application. Thus, to deconvolute an action potential into its components and relate them to pathways or functional categories inside a cell requires some prior knowledge of the biology of the system (i.e., a data base of biological test data on the subject cell culture) in order to perform the deconvolution step and identify cell pathways. A paper we submitted by Mohan, et al. (submitted herewith) illustrates some of our efforts in this area and an implementation of the algorithm shown in Figure 10 of the patent application. This algorithm has been used to deconvolute one of the examples given in Figure 5 of the application and is shown in Figure A, below.

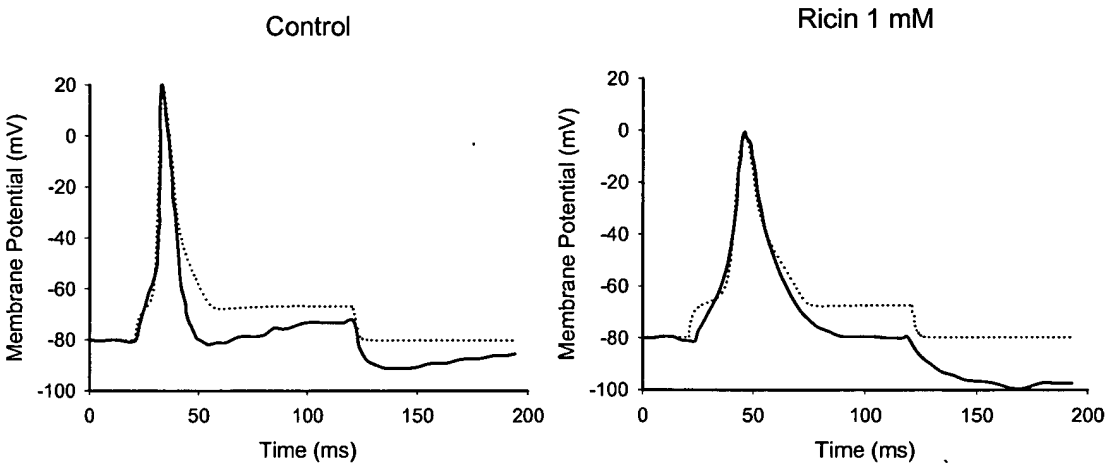

Figure A. Result of parameter fitting to action potential shapes before (left panel) and after (right panel) the application of 1 mM Ricin. Action potentials were recorded from differentiated NG108-15 cells using whole-cell patch clamp method. Action potentials was fitted (dotted lines) with a computer model of NG108-15 cells established based on the measurement of ion channel parameters.

Control	Activation					Inactivation				
	g	V_{Rev}	z	$V_{1/2}$	(	A	z	$V_{1/2}$	(	A
Na	140.00	100.00	6.00	-59.93	-0.45	1.80	-7.48	-70.36	0.42	8.00
K	26.00	-80.00	8.00	-10.00	-0.60	10.00				
Ca	11.00	32.00	4.10	-11.00	-0.67	0.47				
Ricin										
Na	**75.00**	100.00	6.00	-59.93	-0.42	**3.00**	-7.48	-70.36	0.42	**12.00**
K	26.00	-80.00	8.00	-10.00	-0.60	**15.00**				
Ca	11.00	32.00	4.10	-11.00	-0.67	**0.80**				

Table 1. Effect of 1 mM Ricin on the action potential parameters. Action potential parameters were obtained by fitting the parameters of our NG108-15 cell model to the experimental data. 1 mM Ricin caused a significant slow-down of the sodium channel kinetics (parameter A) and a decrease of sodium conductances in the membrane (parameter g). The effect of Ricin on the other ion channels were not so profound, partly because potassium and calcium channels are activated at higher membrane potentials, so their contribution to the Ricin-modified action potential is less (the amplitude of the action potential is smaller, barely reaching 0 mV).

This type of analysis is very different than a spectral analysis "i.e. a Fortier Transform" which arbitrarily assigns combinations of sign waves of different frequencies and amplitudes, to represent the area under a curve. The assignment of the different sign waves is arbitrary and, although it gives a unique signature to a signal, there is no way to relate it to biological information, except through an empirical approach to the testing of drugs or other compounds as well as toxic chemicals.

Claims 51 – 67 and 70 - 73 are rejected under 35 USC 103(a) over Borkholder et al. in view of Georger, Jr. et al.

The Examiner concedes that Borkholder et al. does not specifically disclose an intervening layer, as claimed. Furthermore, it does not disclose or suggest serum-free media. Finally, it does not inherently disclose a deconvolution analysis. Instead it mentions that a "pattern of spectral changes provides a unique *signature* for the compound. Matching the spectral change pattern of a test compound with the spectral change pattern for reference compounds provides a useful method for characterization of channel modulating agents." (Col. 4, lines 15 – 20, emphasis added). This passage describes using the observed changes as a fingerprinting method to associate certain channel-modulating compounds with the observed changes, but that is not the same kind of process as deconvoluting a signal to identify the *contributions of different ion channels* to the signal.

Georger Jr. et al. teaches a method of making biosensors using photolithography placement techniques. It never explicitly states that a high-impedance seal is created or that it would enable deconvolution. For instance, col. 7, lines 58 – 63 does not relate to deconvolution, but at most implies a high-impedance seal. Col. 10, lines 58 – 62 describes manual placement, whereas we deposit the cells by cell culture. At col. 13, lines 19 – 24, the cell culture patterning method is to use fewer steps. The discussions at col 16, line 45 and at col. 10, lines 50 – 65 relate to positioning.

Finally, Georger Jr. et al. uses serum (col. 17, lines 60 – 65) and states at col. 18, lines 9 – 10 that "adhesion is unaffected by serum." Especially where high-throughput screening is involved, the absence of serum is vital.

Claims 51 – 73 are rejected under 35 USC 12, first paragraph, for written description problems. Support for the high-impedance intervening layer allowing deconvolution as claimed is found on page 11, lines 6 – 12.

Claim 51 is rejected under 35 USC 12, first paragraph, on enablement grounds. A positive deconvolution step is now recited.

Claims 51 – 73 are rejected under 35 USC 12, second paragraph, as being indefinite for failure to positively recite a deconvolution step. This has been address by amendment.

Claim 57 has bee clarify with respect to the position of the insulator "surrounding" the electrode.

The dependency of claim 61 has been corrected.

Claim 67 does add a limitation over claim 66 because "known function" and "unknown function" are not the only two possibilities for DNA; some DNA has no function at all.

Claim 73 has been cancelled as redundant in view of amended claim 51.

Applicants submit the case is now in condition for allowance.

The Commissioner is authorized to charge the three-month extension of time, or credit any overpayment, to Deposit Account No. 50-1710.

Respectfully submitted,

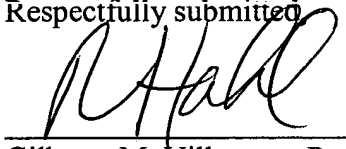

Gilberto M. Villacorta, PH.D.
Registration No. 34,038
Robert W. Hahl, PH.D.
Registration No. 33,893

Attachments: References cited in Remarks by Schaffner *et al.* and Mohan *et al.*

Date: **August 22, 2005**

Patent Administrator
KATTEN MUCHIN ROSENMAN LLP
525 West Monroe Street
Chicago, Illinois 60661-3963
Fax: (312) 906-1021
(202) 625-3500

ELSEVIER

Journal of Neuroscience Methods 62 (1995) 111–119

JOURNAL OF NEUROSCIENCE METHODS

Investigation of the factors necessary for growth of hippocampal neurons in a defined system

Anne E. Schaffner [a,*], Jeffery L. Barker [b], David A. Stenger [b], James J. Hickman [c]

[a] *Laboratory of Neurophysiology, NINDS, NIH, Bldg. 36, Room 2C02, 9000 Rockville Pike, Bethesda, MD 20892, USA*
[b] *Center for Biomolecular Science and Engineering, Code 6090, Naval Research Laboratory, Washington, DC 20375, USA*
[c] *Science Applications International Corporation, 1710 Goodridge Drive, McLean, VA 22102, USA*

Received 3 November 1994; revised 3 April 1995; accepted 21 April 1995

Abstract

We have developed an in vitro system that combines the use of a defined medium with a chemically defined surface for the differentiation of embryonic rat hippocampal neurons. Cells were grown on silica substrates modified with two chemically distinct molecules: poly-D-lysine and an amine-containing organosilane. Cells were dissociated by mechanical or enzymatic methods and grown in serum-containing versus serum-free medium on these surfaces. Our results demonstrate that optimal survival and growth in serum-free medium occurs on the artificial surfaces. X-ray photoelectron spectroscopy (XPS) was used to analyze the surfaces both before and after cell culture. In addition, surface properties such as elemental composition, the initial thickness of the substrate material, and the thickness of material deposited during the course of cell culture were quantified after cell removal. Taken together, the results from the cell culture and surface analysis demonstrate that the media, proteins deposited from the media onto the surface, surface composition, and properties intrinsic to neuronal membranes all interact in a complex fashion to determine whether or not the cells will adhere and survive in culture. In particular, the role of material deposited from the medium onto the culture substratum may be more important than has been previously appreciated. This system allows for the study of neuronal differentiation in a well-defined environment.

Keywords: Neuronal culture; Hippocampus; Rat embryo; X-ray photoelectron spectroscopy; Surface; Serum-free medium; Protein adsorption

1. Introduction

We are investigating the critical parameters involved in the culture of dissociated hippocampal neurons on artificial surfaces. This study has examined several factors that are significant in determining neuronal survival as well as long-term growth and differentiation in vitro including dissociation technique, medium composition and culture substratum. Our approach has been a qualitative assessment of hippocampal neuron viability after varying these parameters, and the quantification of the surface composition and biophysical properties both *before* and *after* cell culture. From the surface quantitative data, we can begin to address the importance of non-specific surface effects on neuronal adhesion and long-term survival in vitro.

Culture of cells dissociated from the embryonic central nervous system (CNS) provides ready access to multi-disciplinary analysis of cellular differentiation and synapse formation. A voluminous literature has accumulated detailing culture conditions suitable for differentiating neurons dissociated from the embryonic CNS. However, the conditions have been chosen primarily in an empirical manner and specifically to study different mechanisms associated with development in vitro. There are practically as many protocols as there are investigators using this strategy. Thus, although monolayers of dissociated neurons have been routine, if not indispensable for investigating a wide variety of cellular and molecular mechanisms critical in CNS development, there is no standard protocol. A number of factors have been identified that are most critical in determining neuronal survival and differentiation in vitro. These include (1) embryonic day of the dissociate, (2) dissociation technique, (3) culture medium composition, and (4) culture substratum (see Banker and Goslin, 1991).

We have investigated three of these variables in the study of embryonic rat hippocampal neurons: dissociation

* Corresponding author: Tel.: (301) 402-1396; Fax: (301) 402-1565.

Elsevier Science B.V.
SSDI 0165-0270(95)00063-1

technique, medium composition and culture substratum. Substrata commonly used for dissociated neuronal cell culture include polymers of basic amino acids (polylysine and polyornithine) (Yavin and Yavin, 1974; Adler and Varon, 1981) and extracellular matrix constituents such as collagen (Elsdale and Bard, 1972; Carbonetto et al., 1983), fibronectin, and laminin (Lein et al., 1992; Lochter and Schachner, 1993). These proteins and amino acid homopolymers promote cell adhesion, neuronal survival, and neurite outgrowth. Extracellular matrix components are presumed to enhance neuronal cell attachment and process formation by interaction with specific receptors on the cell surface (De Curtis, 1991; Clark et al., 1993; Letourneau et al., 1994). Polycationic amino acids are thought to mediate between opposing negative charges on plastic or glass and cell surfaces and thus act as a positively charged bridge (Lieberman and Ove, 1958). Recently, artificial surfaces composed of silane self-assembled monolayers (SAMs) have been shown to support culture of dissociated mammalian neurons (Kleinfeld et al., 1988; Stenger et al., 1993; Hickman et al., 1994). SAM surfaces may be preferable to other types of substrata for reasons that include the wide variety of functional groups available (Ulman, 1991), the ability to modulate the surface free energy (Stenger et al., 1992), and the ability to create geometric patterns without resists or micromachining of the surface (Dulcey et al., 1991; Stenger et al., 1992; Ranieri et al., 1993; Soekarno et al., 1993; Hickman et al., 1994).

While a suitable surface is necessary to promote neuronal growth, it is not sufficient, and other factors, chiefly media components including serum, hormones and trophic factors are required for long-term survival (Cestelli et al., 1992; Stichel and Muller, 1992; Ohsawa et al., 1993; Schmidt and Kater, 1993). The use of serum-free media has enabled the study of neurons in a chemically defined environment (Bottenstein and Sato, 1980; Romijn et al., 1984; Bottenstein, 1985; Romijn, 1988). While studies of in vitro cellular behavior are easier to interpret in well-defined media, it is more difficult to maintain neuronal survival (Romijn, 1988; Ohsawa et al., 1993).

We have examined some of the factors necessary for maintaining embryonic rat hippocampal neurons in vitro in a matrix that compared serum-containing and serum-free media, mechanical and enzymatic dissociation and three different surfaces, poly-D-lysine, EDA, and EDA augmented with heparan sulfate. In the latter case, we looked at the effect of pretreating the surface with the biologically relevant macromolecule, heparan sulfate, as it has been shown to promote neurite outgrowth (Hantaz-Ambroise et al., 1987; Stenger et al., 1993). We have used surface analytical tools such as X-ray photoelectron spectroscopy (XPS) and contact angle measurements to quantify the surface properties both before and after culture. We have related a first-order surface property, the amount of protein adsorption, to cell viability and survival. We propose an hypothesis to explain these observed effects.

2. Materials and methods

2.1. Chemicals

N-2-aminomethyl-3-aminopropyl-trimethoxysilane, (EDA), was used as received from Hüls of America (Petrarch Silanes, Bristol, PA). Heparan sulfate glycosaminoglycan (HS) was obtained from Sigma (St. Louis, MO). High molecular weight poly-D-lysine (PL, 500K) was purchased from Collaborative Research Products (Bedford, MA). Papain and deoxyribonuclease were purchased from Worthington Biochem. (Freehold, NJ). Serum-free additives and trypsin inhibitor (ovomucoid) were purchased from Sigma with the exception of albumin (Miles/Pentex, Kankakee, IL), triiodothyronine and corticosterone (Calbiochem, San Diego, CA).

2.2. Substrate preparation

The PL and organosilane films were deposited on glass coverslips (22 × 22 mm, 0 thickness) purchased from Thomas Scientific (Swedesboro, NJ) or 50 mm diameter n-type polished silicon wafers obtained from Virginia Semiconductor (Fredericksburg, VA). Glass surfaces were first cleaned using HCl/methanol (1:1) followed by a concentrated H_2SO_4 soak for 30 min followed by a water rinse. PL films were deposited by exposing cleaned surfaces for 1 h at room temperature to 20 μg/ml PL dissolved in sterile, tissue culture-grade water. The EDA films were formed by reaction of cleaned surfaces with 1% (v/v) mixtures of the organosilane in 94% (v/v) 1 mM acetic acid in anhydrous methanol and 5% water for 15 min (Hickman et al., 1994). HS at 100 μg/ml in sterile, tissue culture grade water was adsorbed to EDA surfaces by incubation at 36°C for 18 h.

2.3. Preparation of cells

Tissue was derived from the hippocampi of 18–19-day-old rat embryos. Tissue was mechanically dissociated in calcium- and magnesium-free Hank's balanced salt solution, 0.5 mM EDTA and 0.01% deoxyribonuclease (DNase) for approximately 40 min at 37°C. Tissue treated enzymatically was dissociated in Earle's balanced salt solution (EBSS) with 1.0 mM L-cysteine, 0.5 mM EDTA, 0.01% DNase, and 20 U/ml papain under similar conditions (Huettner and Baughman, 1986). After either dissociation method cells were resuspended in 3 ml of EBSS with 0.01% DNase, 1 mg/ml bovine serum albumin (BSA) and 1 mg/ml ovomucoid and overlaid on 5 ml of EBSS containing 10 mg/ml BSA and 10 mg/ml ovomucoid. The 2-step gradient was centrifuged at 80 × *g* for 5 min and effectively removed dead cells and debris. The pellet containing live cells was resuspended in the appropriate plating medium. Cells were plated onto glass coverslips at a density of $3–4 \times 10^4$ cells/cm^2. Cultures were main-

tained in minimal essential medium (MEM) with 5% fetal calf serum (FCS) and 5% horse serum (MEM-S) or in serum-free medium (MEM-N3). Serum-free additives were used according to Romijn et al. (1984). The final concentration of the serum-free components were as follows: BSA, 10 μg/ml; transferrin, 200 μg/ml; putrescine, 200 μM; sodium selenite, 60 nM; triiodothyronine, 20 ng/ml; insulin, 10 μg/ml; progesterone, 40 nM; corticosterone, 40 ng/ml. All cultures were maintained in a humidified atmosphere of 9.5% CO_2 in air at 36°C. At various time points, cells were examined and photographed on a Nikon Diaphot microscope using phase-contrast optics. Each permutation of dissociation method/medium/surface was run in duplicate and, in all cases, the qualitative assessment of neuronal survival and their morphology was the same in duplicate cultures. The cell culture experiment was repeated using two more independent dissociations/platings. The results from all three experiments were similar.

2.4. Wettability measurements

Contact angles were measured by applying static, sessile drops of deionized water to substrate surfaces. A Zisman type goniometer was used to make measurements visually on both sides of the drops. The advancing water contact angle, $\theta_{a(H2O)}$, was taken as the maximum contact angle observed as the drop size was incrementally increased from 5 to 30 μl without an increase in the contact angle. Measured values of $\theta_{a(H2O)}$ for a given film varied by only 3° across the substrate surfaces, implying macroscopically uniform surface coverages. Replicate measurements (≥ 3) were obtained for each modified substrate region.

2.5. X-ray photoelectron spectroscopy measurements

XPS is a technique for the elemental analysis and characterization of surfaces (Briggs and Seah, 1992). Surface analysis was used to define the surface composition both before cell culture and at 10–15 days postplating. For samples to be analyzed by XPS, the silanization was performed either on glass coverslips or polished silicon wafers. XPS data were obtained on a SSX-100 spectrometer equipped with an Al Kα source, quartz monochromator, concentric hemispherical analyzer operating at fixed analyzer transmission mode, and a multichannel detector. The take-off angle was 35° and the operating pressure was less than 10^{-8} Torr. X-ray damage was minimized by limiting acquisition times. All spectra were referenced to the Si $2p_{3/2}$ peak of the substrate and the areas were normalized to the Si peak as well. Sample charging was neutralized with a 2.7 eV electron beam.

2.6. Ellipsometry

The thickness of the material bound to the substrate was determined by ellipsometry. Film thickness measurements were made using a Gaertner Model L115C ellipsometer equipped with a helium–neon laser (632.8 nm) light source. A refractive index of $1.50 \pm 10\%$ was assumed for protein-modified surfaces. Refractive index values have been reported for certain proteins (Prime and Whitesides, 1991) and should not vary much from protein to protein since the component parts are similar. The data obtained by ellipsometry complemented the thickness values obtained by XPS measurements. One advantage of ellipsometry is that surfaces do not need to be dried prior to obtaining the measurement.

3. Results

3.1. Cell survival and growth in vitro

Three surfaces were evaluated for their ability to support neuronal growth: poly-D-lysine (PL), an organosilane (EDA), and an EDA film to which HS had been pre-adsorbed prior to cell culture (EDA/HS). PL is a standard culture substratum and one we selected as our reference material. EDA is a positively charged surface which may mimic PL, and HS is an anionic material that will provide contact to the positively charged EDA (Stenger et al., 1993). Two different cell preparation methods were used (enzymatic and mechanical dissociation), and two types of media were examined (serum-containing and serum-free MEM-N3).

Neurons in culture for 24 h in serum-containing MEM are shown in Fig. 1 and Table 2. PL supported both neuron survival and neurite outgrowth (Fig. 1A,B) while EDA (Fig. 1C,D) and EDA/HS (Fig. 1E,F) modified surfaces did not support neuronal survival or neurite outgrowth regardless of dissociation method. Comparison of dissociation methods shows that surviving cells were mostly aggregated on EDA and EDA/HS after enzymatic treatment (Fig. 1D,F), but were largely dispersed after mechanical dissociation (Fig. 1C,E) although small aggregates were seen here as well.

Neurons in culture for 24 h in serum-free MEM-N3 are shown in Fig. 2 and Table 2. The 6 panels represent the same substratum/dissociation method combinations as in Fig. 1. In contrast to the results in MEM-S, PL did not support survival as well as EDA or EDA/HS; growth on the organosilanes was comparable to that observed for PL with serum. There was virtually no cell survival on PL after enzymatic dissociation although cells did survive and extend processes after mechanical dissociation. Papain treated cells did equally well on EDA or EDA/HS (Fig. 2D,F).

After 72 h, cells continued to be viable and extend neurites on PL in the presence of serum, and on EDA or EDA/HS in serum-free medium. Neurons survived for 7–10 days on EDA or EDA/HS in serum-free medium. Longer survival (> 2 weeks) occurred only on PL in the presence of serum.

3.2. Surface analysis

Surface analysis was used to define the surface composition both before and after cell culture. Prior to cell culture, all substrates were examined by XPS and characterized with respect to contact angle. XPS is a powerful analytical tool since it allows for the identification and the quantitation of the elemental composition of a surface. The

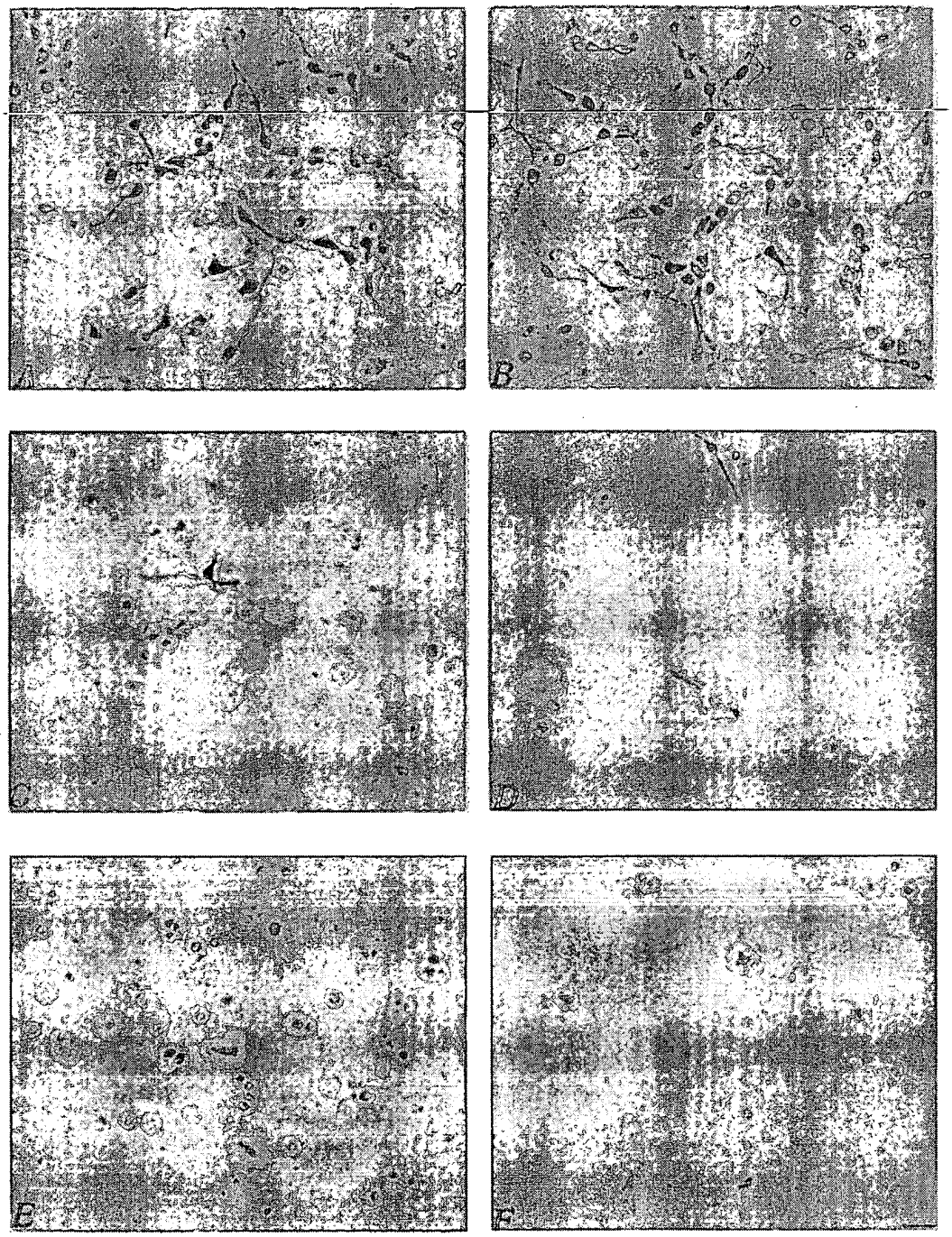

Fig. 1. Hippocampal cells from 18-day-old embryos in culture for 24 h in serum-containing medium. A: cells mechanically dissociated and plated on poly-D-lysine. B: cells dissociated in papain and plated on poly-D-lysine. Cells survived under both conditions and many exhibit processes. C: cells mechanically dissociated and plated on EDA. D: cells dissociated in papain and plated on EDA. Under both conditions survival was dramatically less than on poly-D-lysine and process formation was minimal. Papainized cells appear more clumped than those mechanically dispersed. E: cells mechanically dissociated and plated on EDA/HS. F: cells dissociated in papain and plated on EDA/HS. Survival under these conditions was also poor with minimal process formation. As with EDA alone, papainized cells have clumped more than mechanically dispersed cells.

electrons of each element possess characteristic binding energies. As a result, the energy pattern of emitted photoelectrons arising from a given element serves to unambiguously identify that element, while the precise peak positions or chemical shifts reflect the chemical environment (i.e., oxidation state) in which the element is found. The area under a given peak is proportional to the number of atoms corresponding to that element present in a sample and can be quantified from the known photoionization cross-section of each elemental orbital (Scofield, 1976).

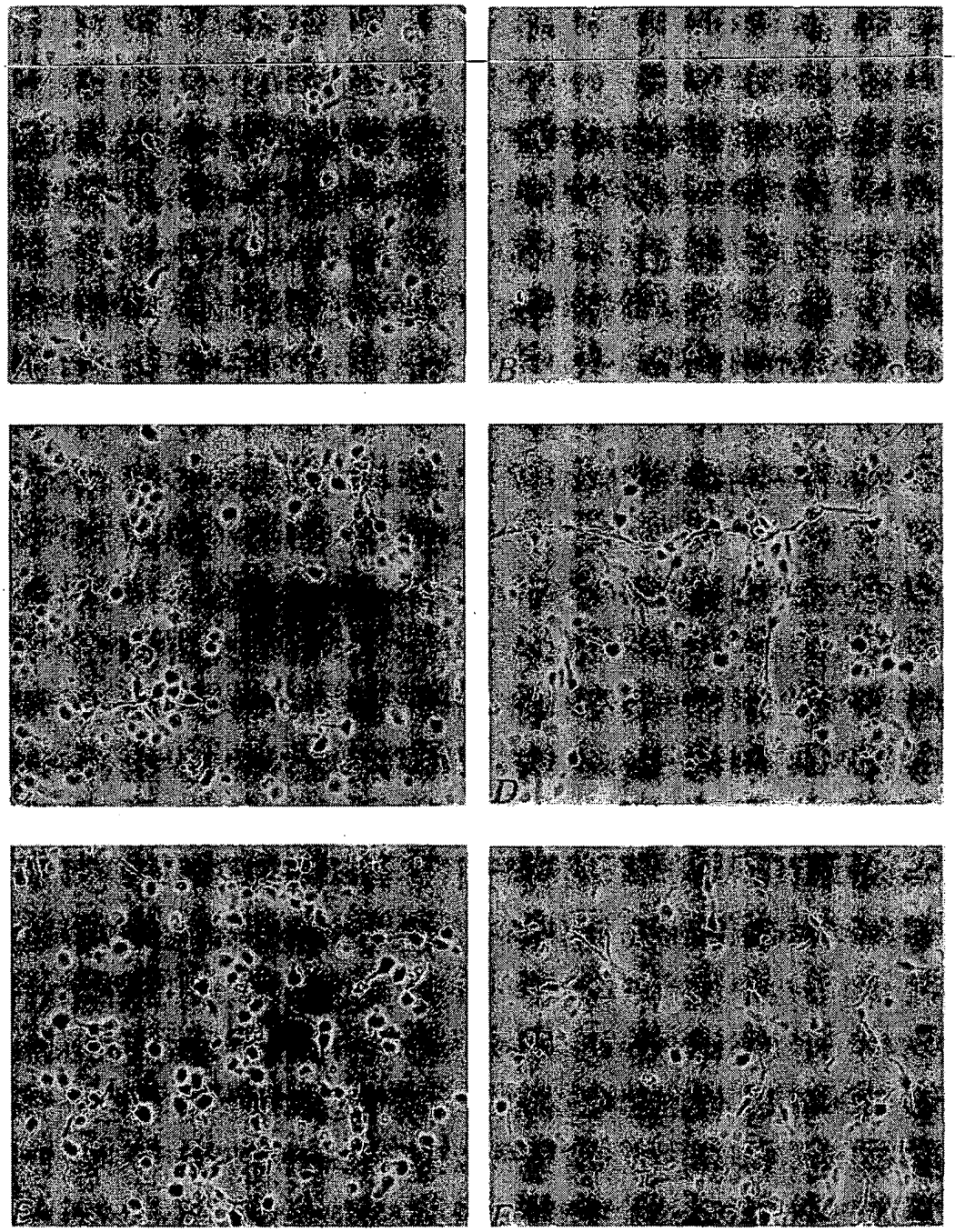

Fig. 2. Hippocampal cells from 18-day-old embryos in culture for 24 h in serum-free medium. A: cells mechanically dissociated on poly-D-lysine. B: cells dissociated with papain on poly-D-lysine. More cells survived and extended processes after mechanical dissociation. C: mechanically dissociated cells on EDA. D: papainized cells on EDA. Cell survival and process formation occurred under both of these conditions. E: mechanically dissociated cells on EDA/HS. F: papainized cells on EDA/HS. Survival was apparent under both conditions; however, there appeared to be more numerous and more highly branched processes on EDA/HS than on EDA alone.

For these experiments, the size of the Si peak is related to the amount of material present on the surface, and can be compared to its magnitude prior to cell culture. In high-resolution scans, the carbon carbonyl peak and the nitrogen signal allow for the preliminary identification of any deposited material as either protein-like or otherwise. As determined by XPS, the ratio of protonated to non-protonated nitrogen signals (401 eV and 399 eV, respectively) indicated that the total surface charge due to the amine groups for EDA and PL was equivalent. XPS in combination with ellipsometry established that the thickness of the PL was 15–20 Å while that of the EDA was 5–7 Å. After incubation with HS, the thickness of the material deposited on the silica substrates was, on average, 2–3 Å thicker, as measured by ellipsometry.

After the culture experiments were concluded, the substrates were vigorously washed with normal saline to remove all the cells (determined by microscopic observation) followed by three rinses in distilled water to remove

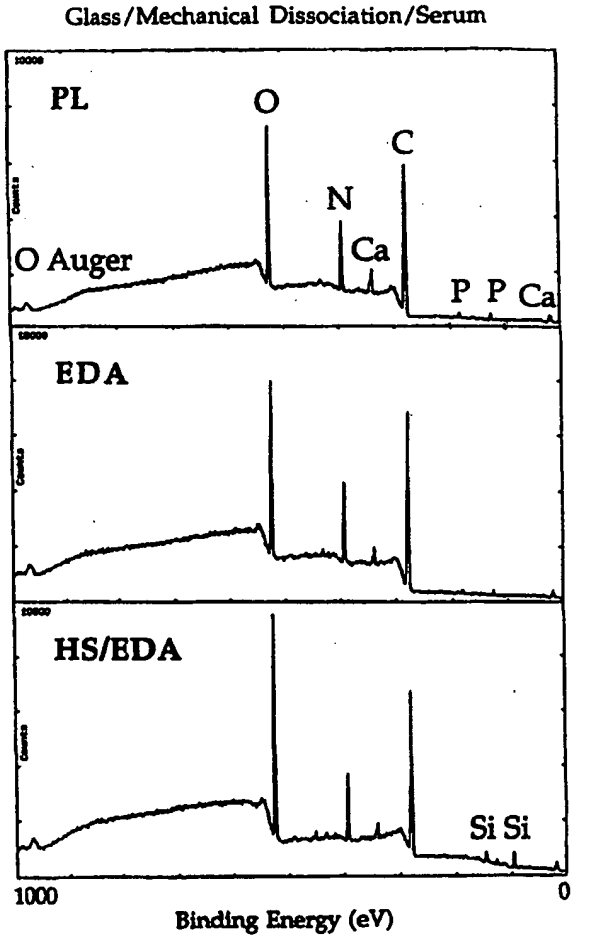

Fig. 3. XPS survey spectra of the culture plates in serum-containing medium. The plates analyzed were the same as those depicted in Fig. 1 after removal of the cells. (Top) Poly-D-lysine-coated glass. (Middle) EDA-only-derivatized glass. (Bottom) EDA/HS-derivatized glass. Note that the Si signal is greatest in the bottom panel.

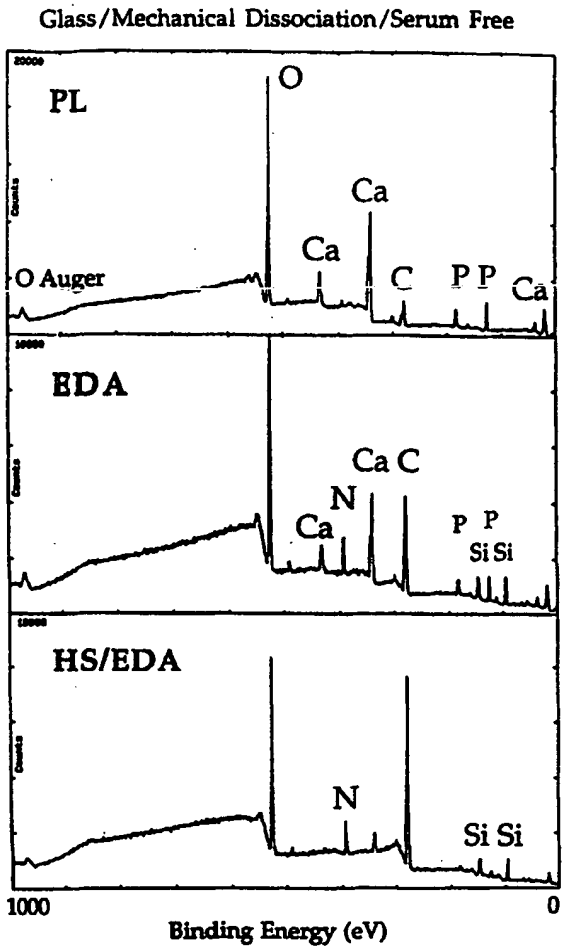

Fig. 4. XPS survey spectra of plates in serum-free culture conditions. The plates analyzed were the same as those depicted in Fig. 2 after removal of the cells. (Top) Poly-D-lysine-coated glass. (Middle) EDA-only-derivatized glass. (Bottom) EDA/HS-derivatized glass. Note from the size of the Si peak that the amount of adsorbed material is much less on the serum-free culture plates than on the serum-containing culture plates. Also note that EDA/HS has the least amount of adsorbed material.

loosely bound salts, and then re-examined by XPS. Survey scans for the elements were obtained by XPS, and illustrate the differences in the amounts of certain elements on the surfaces after culture in serum (Fig. 3) and in serum-free medium (Fig. 4). In MEM-S, the relative amounts of carbon (C), oxygen (O), and nitrogen (N) were the same on all three surfaces (Fig. 3). Phosphorus (P) and calcium (Ca) could also be detected. In contrast, Fig. 4 shows that the relative amounts of C, O, N, P, and Ca were different for each surface when cells were cultured in serum-free medium.

Another difference revealed by XPS was that the amount or thickness of material on the EDA/HS surfaces (Fig. 3 and 4, bottom panel) was less than on PL (Fig. 3 and 4, top panel) indicating that HS may be preventing media components, most likely proteins, from adsorbing to the surface. This reduction in adsorbed material did not neces-

Table 1
Relative thickness of Si material deposited from culture media onto glass coverslips measured by XPS

	PL	EDA	EDA/HS
Serum Papain	–	140	323
Serum Mechanical	–	54	495
Serum-free Papain	506	1043	929
Serum-free Mechanical	75	686	512

Shown is the relative size of the Si 2p XPS peak after cell culture of hippocampal neurons under a variety of culture conditions. The smaller the Si peak, the larger the amount of protein adsorption. The peak sizes are in arbitrary units. Abbreviations: PL, poly-D-lysine; EDA, N-2-aminomethyl-3-aminopropyl-trimethoxysilane; HS/EDA, heparan sulfate adsorbed to EDA prior to cell culture. The values are an average of two trials with three analyses per trial.

sarily correlate with cell survival. The amount of adsorbed material on EDA was markedly different in the two types of media, i.e., serum-containing and serum-free (Fig. 3 and 4, middle panel), and this did correspond to cell survival. The relative amount of material on a surface can be deduced from the magnitude of the silicon peak at 102 eV resulting from the underlying silica substrate. The data in Table 1 indicate the relative magnitude of the Si 2p peak for each permutation of cell culture condition. It is evident from the relatively small Si peaks for PL in serum-containing medium that there were thicker adsorbed layers on this substrate, which ensured neuronal viability, while neurons did not survive on the amine-containing monolayer, EDA, that contained nearly as thick a deposition (Fig. 3 and Table 1 and 2). In serum-free conditions mechanically dissociated neurons survived and extended processes on PL while papain-treated neurons were not viable on PL. Again, survival on PL was associated with a thicker adsorbed layer. It should be noted that the *absence* of a thick coating appeared to be related to enhanced cell viability on the silane monolayer films. This is not uniformly adhered to, as in the case of EDA/HS in serum-containing medium where the HS appeared to block protein adsorption but did not promote cell survival.

Thus, we did not observe a one-to-one correlation between thickness or composition and cell survival in any of the conditions we investigated. Clearly there are other factors involved that need to be considered.

Table 2
Qualitative assessment of neuronal survival and growth under various conditions after 24 hours in vitro

	M	P	M	P
P-D-L	+++,*	+++,*	++	+/–
EDA	–	–	+++,*	+++,*
EDA/HS	–	–	+++,*	+++,*
	Medium with serum		Serum-free N3	

A qualitative assessment of both hippocampal cell survival and neurite outgrowth on three different surfaces under different conditions after 24 h in vitro. –, poor; + to +++, fair to very good; *, cells surviving at 1 week in vitro. Abbreviations: PL, poly-D-lysine; EDA, N-2-aminomethyl-3-aminopropyl-trimethoxysilane; EDA/HS, heparan sulfate adsorbed to EDA prior to cell culture; M, mechanically dissociated; P, enzymatically dissociated using papain.

4. Discussion

We have developed a neuronal culture system where critical elements, surface and medium, are well defined and sustain cell survival and differentiation. This is the first systematic study looking at survival and growth of embryonic hippocampal neurons using SAM-modified surfaces as the culture substratum while varying the growth medium and cell dissociation method. We compared the ability of polylysine, a standard culture substratum, and an amine-containing silane monolayer to support the growth and differentiation of primary hippocampal neurons in vitro under a variety of conditions. In addition the silane monolayer was augmented with an anionic biological macromolecule, heparan sulfate.

We combined the cell culture experiments with quantitative surface analysis to measure the reproducibility of surface preparation within a single experiment and from experiment to experiment. We found that the elemental composition of the surface was invariant from experiment to experiment, and that relatively similar amounts of material were deposited onto the surfaces during cell culture. We correlated surface properties with cell survival and differentiation in order to determine how the surface could influence neuronal behavior. Possible mechanisms included the following: (1) different surfaces may dictate different deposition profiles of biological macromolecules from the culture media, and these could be governing the interaction; (2) the surface may send signals into the cell with little resultant change in the material outside the cell; or (3) the cell may receive signals from the surface and therefore begin to synthesize a different extracellular matrix.

Hippocampal neurons survived in MEM-S but only on PL. Examination of the relative distribution of elements on the three surfaces after cell culture showed few, if any, differences (see Fig. 3). The only apparent difference was the thickness of the deposited material; from the size of the Si peaks, there was less material on the EDA/HS surface than on either PL or EDA alone. Culturing hippocampal neurons in serum-free medium on the same three surfaces resulted in dramatically different cell growth trends. After 24 h in culture, cells survived poorly on PL especially after enzymatic dissociation, and much better on EDA or EDA/HS. In contrast to the results seen in MEM-S, there were many differences among the three surface compositions after cell culture in MEM-N3. We conclude from

these results that an artificial surface combined with a defined medium optimizes for growth and differentiation of hippocampal neurons. This strategy provides a baseline for the development of an in vitro assay system for hippocampal culture and ultimately the development of neuronal networks.

The results of the surface analysis, in addition to establishing a baseline that will yield a reproducible in vitro system, also begins to address mechanistic questions regarding events occurring at the cell/surface interface during cell culture. In serum-containing medium, the elements associated with protein adsorption (C,N,O) and their relative abundance were indistinguishable on PL, EDA, or EDA/HS despite dramatic differences in the ability of these surfaces to support neuronal growth. One difference we did observe was that there was far more material deposited on the PL and EDA surfaces than on the HS/EDA-modified surface. However, this points out an extremely important point that if the thickness is similar on EDA as well as PL then the composition or state of the adsorbed proteins *must* be different based on the differences in cell survival. It is possible that the types of proteins within the adsorbed layer is the result of differential adsorption onto the surface from the medium.

The results in serum-free medium are more difficult to interpret since the elemental distributions are different on each surface. Our study suggests that, in the absence of serum, the substratum may play a more dominant role in defining the nature of the cell/surface interaction. This is because the relative amounts of C, O, N, and P were different for EDA and PL surfaces when cells were cultured in serum-free medium. The lower amount of material deposited on EDA/HS surfaces suggests that the HS may be preventing proteins from adsorbing to the surface. We again observed that the thickest layer of deposited material was on PL, yet in MEM-N3, this was the worst substratum. Both the EDA and EDA/HS surfaces supported neuronal viability and had similar (thinner) adsorbed layers. These results together suggest the following scenario: the nature of the surface may dictate what material is deposited from the medium (or is secreted by the cells) during the course of cell culture. Thus, modified surfaces exposed to different media components (i.e., those of MEM-S or MEM-N3) would be coated with different biomolecules, predominantly proteins and ions, and the neurons' response to the surface would then be dictated by the nature of the deposited material (see Fig. 5). The *thickness* of the deposited material is not the single controlling variable, nor is the nature of the surface beneath the deposited material (since PL and EDA/HS have opposite effects in different serum combinations); it is also unlikely that the plated cells are able to 'sense' the substratum underneath 50–100 Å of deposited material.

We believe the situation is similar to that depicted in the cartoon in Fig. 5. Adsorption of proteins onto the surface of biomaterials involves conformational rearrangement that can result in denaturation (Pusineri and Cazenave, 1986; Brash, 1992). We postulate that less protein denaturation occurs on the monolayer surfaces. Polyanions such as heparan sulfate are known to prevent denaturation of proteins (Burke et al., 1993). Monolayers might prevent denaturation because they could be more difficult to dehydrate than PL. The absence of denatured material on a surface would enhance cell survival. A related hypothesis is that in serum-containing medium, denatured material is deposited on EDA but in serum-free medium this does not occur. This hypothesis would further require that denaturation also occurs on PL but not enough to prevent cell survival. This may account for the fact that it has become a standard culture substratum.

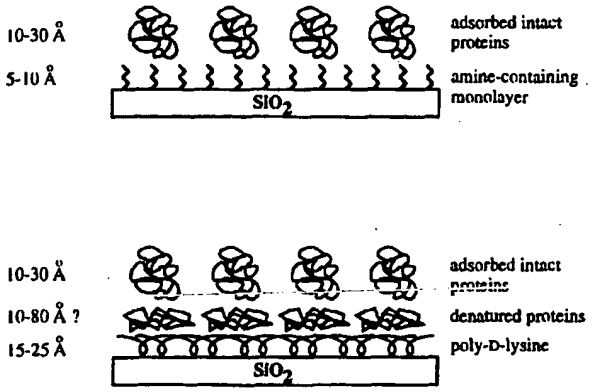

Fig. 5. A schematic depicting our hypothesis on the effect of surface composition on protein structure. The top panel shows a self-assembled monolayer on glass with a thin layer of adsorbed protein with structure intact. The bottom panel shows poly-D-lysine on the surface with the deposition of a much thicker layer of proteinaceous material. PL would have caused the initial adsorbed protein layer to denature.

It is also of interest to note the differences observed between mechanically and enzymatically dissociated cells. In serum-containing medium the cells on EDA and EDA/HS clumped after enzymatic dissociation but not after mechanical dissociation indicating that for adhesion to the surface, components of the plasma membrane are important. If they are removed, cells adhere to each other more readily than to the surface. It appears that PL enables the establishment of a number of acceptable surfaces for cell growth in different media or establishes the same surface even in a variety of media conditions. This could be accomplished via selective adsorption of a particular macromolecule, present in most media, that requires a specific or non-specific interaction with some membrane component of the cell. Enzymatic dissociation in serum-free medium must remove something from the neuronal surface that is necessary for this interaction (and is not available in medium); hence, survival of the neurons is compromised.

This study indicates that at present, we can control and quantify an artificial surface while maintaining cells in a defined medium making it easier to elucidate cell/surface interactions. Since the hippocampus is the brain region

critical to cognitive functions such as learning and memory and is the focus of seizure activity, understanding how discrete regions of the hippocampus form and what factors control synaptogenesis are some of the challenging issues in developmental neurobiology. Ultimately, we hope to create a system of patterned hippocampal networks and study neuronal behavior in a defined and reproducible environment.

Acknowledgements

James J. Hickman was supported by an SAIC Internal Research and Development grant and NICHD Grant ROI-HD31457-2.

References

Adler, R. and Varon, S. (1981) Neuritic guidance by polyornithine-attached materials of ganglionic origin, Dev. Biol., 81: 1–11.

Banker, G. and Goslin, K. (1991) Culturing Nerve Cells. In: C.F. Stevens (Ed.), Cellular and Molecular Neuroscience Series. The MIT Press, Cambridge, MA.

Bottenstein, J.E. (1985) Growth and differentiation of neural cells in defined media. In: J.E. Bottenstein and G. Sato (Eds.), Cell Culture in the Neurosciences, Plenum Press, New York, pp. 3–43.

Bottenstein, J.E. and Sato, G.H. (1980) Fibronectin and polylysine requirement for proliferation of neuroblastoma cells in defined medium, Exp. Cell Res., 129: 361–366.

Brash, J.L. (1992) Role of plasma protein adsorption in the response of blood to foreign surfaces. In: C.P. Sharma and M. Szycher (Eds.), Blood Compatible Materials and Devices: Perspectives Towards the 21st Century, Technomic Publ., Lancaster, PA, pp. 3–24.

Briggs, M.P. and Seah, M.P. (1992) Practical Surface Analysis by Auger and X-ray Photoelectron Spectroscopy, John Wiley, New York.

Burke, C., Volkin, D., Mach, H. and Middaugh, C. (1993) Effect of polyanions on the unfolding of acidic fibroblast growth factor, Biochemistry, 32: 6419–6426.

Carbonetto, S., Gruver, M.M.S. and Turner, D.C. (1983) Nerve fiber growth in culture on fibronectin, collagen, and glycosaminoglycan substrates, J. Neurosci., 3: 2324–2335.

Cestelli, A., Savettieri, G., Salemi, G. and Di Liegro, I. (1992) Neuronal cell cultures: a tool for investigations in developmental biology, Neurochem. Res., 17: 1163–1180.

Clark, P., Britland, S. and Connolly, P. (1993) Growth cone guidance and neuron morphology on micropatterned laminin surfaces, J. Cell Sci., 105: 203–212.

De Curtis, I. (1991) Neuronal interactions with the extracellular matrix, Curr. Opin. Cell Biol., 3: 824–831.

Dulcey, C.S., Georger, J., Jr., Krauthamer, V., Stenger, D.A., Fare, T.L. and Calvert, J.M. (1991) Deep UV photochemistry of chemisorbed monolayers: patterned coplanar molecular assemblies, Science, 252: 551–4.

Elsdale, T. and Bard, J. (1972) Collagen substrata for studies on cell behavior, J. Cell Biol., 54: 626–637.

Hantaz-Ambroise, D., Vigny, M. and Koenig, J. (1987) Heparan sulfate proteoglycan and laminin mediate two different types of neurite outgrowth, J. Neurosci., 7: 2293–2304.

Hickman, J.J., Bhatia, S.K., Quong, J.N., Shoen, P., Stenger, D.A., Pike, C.J. and Cotman, C.W. (1994) Rational pattern design for in vitro cellular networks using surface photochemistry, J. Vac. Sci. Technol. A, 12: 607–616.

Huettner, J.E. and Baughman, R.W. (1986) Primary culture of identified neurons from the visual cortex of postnatal rats, J. Neurosci., 6: 3044–3060.

Kleinfeld, D., Kahler, K.H. and Hockberger, P.E. (1988) Controlled outgrowth of dissociated neurons on patterned substrates, J. Neurosci., 8: 4098–4120.

Lein, P.J., Banker, G.A. and Higgins, D. (1992) Laminin selectively enhances axonal growth and accelerates the development of polarity by hippocampal neurons in culture, Dev. Brain Res., 69: 191–197.

Letourneau, P.C., Condic, M.L. and Snow, D.M. (1994) Interactions of developing neurons with the extracellular matrix, J. Neurosci., 14: 915–928.

Lieberman, I. and Ove, P. (1958) A protein factor for mammalian cells in culture, J. Biol. Chem., 233: 637.

Lochter, A. and Schachner, M. (1993) Tenascin and extracellular matrix glycoproteins: from promotion to polarization of neurite growth in vitro, J. Neurosci., 13: 3986–4000.

Ohsawa, F., Widmer, H.R., Knusel, B., Denton, T.L. and Hefti, F. (1993) Response of embryonic rat hippocampal neurons in culture to neurotrophin-3, brain-derived neurotrophic factor and basic fibroblast growth factor, Neuroscience, 57: 67–77.

Prime, K.L. and Whitesides, G.M. (1991) Self-assembled organic monolayers: model systems for studying adsorption of proteins at surfaces, Science, 252: 1164–1167.

Pusineri, C. and Cazenave, J.-P. (1986) Adsorption at interfaces. In: J.-P. Cazenave, J.A. Davies, M.D. Kazatchkine and W.G. van Aken (Eds.), Blood-Surface Interactions: Biological Principles Underlying Haemocompatability with Artificial Materials. Elsevier, Amsterdam, pp. 45–59.

Ranieri, J.P., Bellamkonda, R., Jacob, J., Vargo, T.G., Gardella, J.A. and Aebischer, P. (1993) Selective neuronal cell attachment to a covalently patterned monoamine on fluorinated ethylene propylene films, J. Biomed. Mat. Res., 27: 917–925.

Romijn, H.J. (1988) Development and advantages of serum-free, chemically defined nutrient media for culturing of nerve tissue, Biol. Cell, 63: 263–268.

Romijn, H.J. van Huizen, F., and Wolters, P.S. (1984) Towards an improved serum-free, chemically defined medium for long-term culturing of cerebral cortex tissue, Neurosci. Biobehav. Rev., 8: 301–334.

Schmidt, M.F. and Kater, S.B. (1993) Fibroblast growth factors, depolarization, and substratum interact in a combinatorial way to promote neuronal survival, Dev. Biol., 158: 228–237.

Scofield, J.H. (1976) Hartree-Slater subshell photoionization cross-sections at 1254 and 1487 eV. J. Electron Spect. Rel. Phenom., 8: 129–137.

Soekamo, A., Lom, B. and Hockberger, P.E. (1993) Pathfinding by neuroblastoma cells in culture is directed by preferential adhesion to positively charged surfaces, Neuroimage, 1: 129–144.

Stenger, D.A., Georger, J.H., Dulcey, C.S., Hickman, J.J., Rudolph, A.S., Nielsen, T.B., McCort, S.M. and Calvert, J.M. (1992) Coplanar molecular assemblies of amino- and perfluorinated alkylsilanes: characterization and geometric definition of mammalian cell adhesion and growth, J. Am. Chem. Soc., 114: 8435–8442.

Stenger, D.A., Pike, C.J., Hickman, J.J. and Cotman, C.W. (1993) Surface determinants of neuronal survival and growth on self-assembled monolayers in culture, Brain Res., 630: 136–147.

Stichel, C.C. and Muller, H.W. (1992) Expression of inherent neuronal shape characteristics after transient sensitivity to epigenetic factors, Dev. Brain Res., 68: 149–162.

Ulman, A. (1991) Introduction to Ultrathin Organic Films, Academic Press, San Diego, CA.

Yavin, E. and Yavin, Z. (1974) Attachment and culture of dissociated cells from rat embryo cerebral hemispheres on polylysine-coated surface, J. Cell Biol., 62: 540–546.

Title: Toxin detection based on action potential shape analysis using a realistic mathematical model of differentiated NG108-15 cells

Authors: Dinesh K Mohan[2], Peter Molnar[1,2] and James J. Hickman[1,2*,]

[1]Nanoscience Technology Center, University of Central Florida, Orlando, FL 32826,

[2]Department of Electrical Engineering, Clemson University, Clemson, SC 29634, U.S.A

*Corresponding Author

Address:

12424 Research Parkway, Suite 400

Orlando, FL 32826

Phone: (864) 710 8472

Fax: (407 882 1156

E-mail: jhickman@mail.ucf.edu

Introduction

In the areas of environmental protection, toxicology and drug development there are increasing demands for high-throughput functional screening methods (Rogers 1995; Paddle 1996; Ohlstein, Ruffolo et al. 2000; Heck, Roy et al. 2001; Croston 2002; Tzoris, Fearnside et al. 2002). For monitoring of the environment, whole-cell biosensors could be more effective than physico-chemical methods to assess the global toxicity of the wide variety of chemicals that are possible pollutants (Evans, Briers et al. 1986; Rogers 1995; Bousse 1996; Paddle 1996; Naessens and Tran-Minh 1998). Whole-cell biosensors are also able to give functional information about the effect of chemicals, have the ability to detect unknown compounds and continuous monitoring of external conditions is possible as they can be made small enough to allow field applications (Bousse 1996). Another benefit of whole cells in environmental applications is that they allow the measurement of the total bioavailability of a given pollutant rather than its free form (Bousse 1996; Naessens and Tran-Minh 1998; Philp, Balmand et al. 2003). Similarly, in safety pharmacology, the side effect spectrum of a given compound is not known, thus, the application of complex functional tests at the whole-organism-level are necessary (Jorkasky 1998; Kinter and Valentin 2002) and could be addressed with this technique. Moreover, the availability of genomic information significantly increased the number of potential targets available for drug discovery and new methods are necessary for high-throughput functional screening for target validation (Ohlstein, Ruffolo et al. 2000; Croston 2002).

Recently, the application of whole-cell biosensors for toxin detection and drug screening has become more readily accepted (Bousse 1996; Bentleya, Atkinsona et al.

2001; Baeumner 2003) as it has many benefits compared to traditional methods of evaluation. Several techniques have been developed to quantify the physiological changes induced by chemicals in whole-cell biosensors (Bousse 1996; Bentleya, Atkinsona et al. 2001). One of these techniques, which is frequently used for monitoring the physiological state / activity of excitable cells, is multi-electrode extracellular recording of membrane potential (Bousse 1996; Gross, Harsch et al. 1997; Denyer, Riehle et al. 1998; Jung, Cuttino et al. 1998; Offenhausser and Knoll 2001; Krause, Ingebrandt et al. 2000; Stett, Egert et al. 2003). The high-throughput or long-term application of extracellular recording is much preferred over intracellular action potential recording for many applications because the use of an intra-cellular or patch clamp electrode limits the life of the cell to a few hours as does the use of voltage sensitive dyes (all dyes reported to date, to a greater or lesser extent, are toxic to cells) (Mason 1993; Chiappalone, Vato et al. 2003).

Action potential generation and the shape of the action potential depends on the status of several ion channels located in a cell's membrane, which are regulated by receptors and intracellular messenger systems (Gross, Rhoades et al. 1995; Gross, Harsch et al. 1997; Morefield, Keefer et al. 2000). Changes in the extracellular (receptor activation) or intracellular environment (gene expression), in many cases, can be reflected in an alteration of spontaneous firing properties such as the frequency and firing pattern (Gross, Harsch et al. 1997; Amigo, Szczepanski et al. 2003; Chiappalone, Vato et al. 2003; Xia, Gopal et al. 2003) of excitable cells and also in changes in the shape of their action potentials (Clark, Bouchard et al. 1993; Muraki, Imaizumi et al. 1994; Akay, Mazza et al. 1998; Nygren, Fiset et al. 1998; Djouhri and Lawson 1999). There are many

examples indicating that the shape of action potential depends on the extracellular and intracellular environment of the cells. Sodium (Spencer, Yuill et al. 2001), potassium (Clark, Bouchard et al. 1993; Martin-Caraballo and Greer 2000) and calcium channel modulators (Ahmed, Hopkins et al. 1993; van Soest and Kits 1998), as well as several toxins and various pathological conditions (Muraki, Imaizumi et al. 1994; Shaw and Rudy 1997; Akay, Mazza et al. 1998; Djouhri and Lawson 1999) have already been shown to affect the shape of action potentials. However, action potential shape analysis for high-throughput screening applications, such as toxin detection or drug screening, has not yet been developed. Two primary reasons this type of analysis has been lacking to date is that it is difficult to obtain high fidelity recordings from chip-based extracellular electrodes and from the lack of models to adequately analyze the signals.

Several mathematical models have been developed to describe the electrical properties and the process of action potential generation in excitable cells (Agin 1972; Cohen 1976; Otten 1995; Dokos 1996; Weiss 1996; Shevtsova 2003). The most widely used is the Hodgkin-Huxley formalism where ion channel activation and inactivation is described using voltage dependent activation and inactivation gates (Weiss 1996). In the original model the voltage and time dependence of the gates was given utilizing rate constants, which were taken as an empirical function of the membrane potential (Hodgkin.L.A and Huxley.F.A 1952). However, in lieu of using empirical functions, it is also possible to deduce the functional form of the voltage dependence of the rate constants from thermodynamics (Weiss 1996; Destexhe and Huguenard 2000). The applications of these models to extracellular recordings from a suitable excitable cell

population, in combination with the proper models, would be a logical next step in adapting this technology to high throughput toxin detection and drug discovery.

The NG108-15 hybrid cell line, which was created by merging mouse neuroblastoma and rat glioma cells, has been widely used in *in vitro* experiments as a substitute for primary-cultured neurons (Hu, Huang et al. 1997; Doebler 2000; Tojima, Yamane et al. 2000). The neuronal functions and features of differentiated NG108-15 cells have been well characterized, e.g. the presence of a wide range of voltage dependent and transmitter activated membrane currents have been detected as well as second messengers and enzymes normally found in primary neurons (Schmitt and Meves 1995; Lukyanetz 1998; Ma, Pancrazio et al. 1998; Tojima, Yamane et al. 2000). NG108-15 cells are widely used in pharmacology (Hu, Huang et al. 1997) and also as a whole-cell biosensor for toxin detection (Ma, Pancrazio et al. 1998). One of the distinctive features of the NG108-15 cell line, which makes it ideal for whole-cell biosensor applications, is that the cells do not form synaptic connections, thus network activity does not influence single cell data (Ma, Grant et al. 1999).

In this study we created a computer model of the action potential generation of an NG108-15 cell based on voltage-clamp and current clamp electrophysiological recordings. Using this model we developed and demonstrated the applicability of action potential shape analysis as a method for toxin detection and monitoring the physiological state of excitable cells.

Methods

Surface chemistry

NG108-15 cells were plated on N-1[3-(trimethoxysilyl) propyl]diethylenetriamine (DETA) coated glass coverslips (22x22mm, Thomas Scientific). The DETA coated coverslips were prepared according to published protocols (Schaffner, Barker et al. 1995). In brief, glass coverslips were cleaned using HCl/methanol (1:1) followed by a concentrated H_2SO_4 soak for 30 min followed by a water rinse. The coverslips were then boiled in deionized water followed by a rinse with acetone and then oven dried. The DETA films were formed by the reaction of the cleaned surfaces with a 0.1% (v/v) mixture of the organosilane in toluene. The DETA cover glasses were heated to just below the boiling point of toluene, rinsed with toluene; reheated to just below the boiling temperature again and then oven dried.

Culture of NG108-15 cells

The NG108-15 cell line (passage number 16) was obtained from Dr. M. W. Nirenberg (NIH). The NG108-15 cells were cultured according to published protocols (Higashida, Streaty et al. 1986; Ma, Pancrazio et al. 1998). Briefly, the cell stock was grown in T-25 and T-75 flasks in 90% Dulbecco's modified Eagle's medium (DMEM, GIBCO) supplemented with 10% Fetal Bovine Serum and HAT supplement (GIBCO, 100x) at 37°C with 10% CO_2. Differentiation was induced by plating the cells in a serum-free defined medium (DMEM+N2 supplement, GIBCO) in 35mm culture dishes at a density of 40,000 cells/dish.

Electrophysiological recordings

Whole-cell patch clamp recordings were performed in a recording chamber on the stage of a Zeiss Axioscope 2 FS Plus upright microscope. The chamber was continuously perfused (2 ml/min) with the extracellular solution. The composition of the extracellular solution for the recording of action potentials was (in mM): NaCl 140, KCl 3.5, $MgCl_2$ 2, $CaCl_2$ 2, Glucose 10, HEPES 10. For the recording of potassium currents 1 μM tetrodotoxin (TTX) was added to the extracellular solution. To minimize space-clamp errors, sodium currents were recorded in a 'decreased sodium' extracellular solution containing (in mM): NaCl 50, TEA-Cl 100, CsCl 5, $CaCl_2$ 1, $CoCl_2$ 1, $MgCl_2$ 1, Glucose 10, HEPES 10. For the recording of calcium currents, sodium and potassium channels were blocked with Cs, TEA and TTX. The extracellular solution composition for the measurement of calcium currents was (in mM): NaCl 100, TEA-Cl 30, $CaCl_2$ 10, $MgCl_2$ 2, Glucose 10, HEPES 10, TTX 0.001. The pH was adjusted to 7.3 and the osmolarity was 320 mOsm. The intracellular solutions composition for recording the action potentials and for potassium channel measurements was (in mM): Kgluconate 130, $MgCl_2$ 2, EGTA 1, HEPES 15, ATP 5, for sodium channels was CsF 130, NaCl 10, TEA-Cl 10, $MgCl_2$ 2, EGTA 1, HEPES 10, ATP 5 and for calcium channels was: CsCl 120, TEA-Cl 20, $MgCl_2$ 2, EGTA 1, HEPES 10, ATP 5 (pH = 7.2; osmolarity = 280 mOsm). For selecting L-type calcium channels, 1 μM ωCTxGVIA was used.

Patch pipettes (4-6 Mohm resistance) were prepared from borosilicate glass (BF150-86-10; Sutter, Novato, CA) with a Sutter P97 pipette puller. Voltage clamp and current clamp experiments were performed with a Multiclamp 700A (Axon, Union City, CA) amplifier. Signals were filtered at 2 kHz and digitized at 20 kHz with an Axon

Digidata 1322A interface. Data recording and analysis was performed using pClamp 8 (Axon) software. Sodium and potassium currents were measured in voltage clamp mode using voltage steps from a – 85 mV holding potential. To record high-threshold calcium currents, a – 40 mV holding was used. Whole cell capacitance and series resistance was compensated and a p/6 protocol was used. The access resistance was less than 22 Mohm. Action potentials were measured in current-clamp mode using 1 s depolarizing current injections. Data was saved in text-format and imported into MATLAB for further analysis.

Simulation of ionic conductance's and action potential generation in NG108-15 cells.

The classic Hodgkin-Huxley model (Hodgkin.L.A and Huxley.F.A 1952) was used for the description of the ion channel currents, but instead of the original empirical description of the rate constant, the thermodynamic approach (Weiss, Urbaszek et al. 1995; Destexhe and Huguenard 2000) was applied. Briefly, the total ionic membrane current was described as:

$$\mathbf{Iionic} = I_{Na}+I_K+I_{Ca}+I_l = g_{Na}m^3\,h\,(V- V_{Na})+ g_K\,n^4\,(V- V_K)+ g_{CaL}\,e^3\,(V- V_{CaL}) + g_l\,(V- V_l).$$

Dynamic changes in the membrane-potential were calculated according to:

$$\mathbf{dV/dt = (Iexternal - Iionic)/C_M}.$$

The dynamics of the state variables was given as $dm/dt = (m_\infty - m)/\tau_m$. Where g_{Na}, g_K, g_{CaL}, V_{Na}, V_K, V_{CaL} are constants; **m, n, h, e** are the state variables, m_∞, n_∞, h_∞, e_∞ are the steady-state values of the state variables and the τ-s are their voltage-dependent time-

constants. The voltage-dependence of the steady-state state parameters and the time constants were given using the general thermodynamic formalism:

$$m_\infty = 1/(1+\exp(-zF/RT\ (Vm-V_{1/2})))\ \text{and}$$

$$\tau_m = A/((\exp(zF/RT)(\xi(Vm-V_{1/2}))) *(\cosh((zF/2RT)(Vm-V_{1/2})))$$

Where **z**, $V_{1/2}$, **A** and ξ are constants and **Vm** represents the membrane potential. Sodium, potassium and calcium channel mediated currents, which were recorded in voltage-clamp mode at different membrane potentials, were fitted using the built-in routines (fminunc) of MATLAB through a custom-made graphical interface. Parameters obtained from different cells were averaged (n = 4-6) and considered as initial values for the action potential modeling. Simulated action potentials were fitted to the experimental data using built-in functions in MATLAB.

Results

The NG108-15 cells completed their differentiation process and a neuronal phenotype was obtained by day 10 *in vitro* (DIV) in the defined, serum-free medium (Figure 1A). Electrophysiological experiments were performed on the differentiated cells between day 10 and 14 *in vitro*. All of the cells investigated showed pronounced sodium, potassium and calcium currents in the voltage-clamp experiments. Most of the cells fired one single action potential upon depolarization in current-clamp mode, whereas about 10% of the cells were able to fire multiple action potentials. Only a very small minority of the cells (about 5%) were spontaneously active.

Extracting ion-channel parameters from the voltage-clamp experiments using the linear thermodynamic description

Signals from sodium, potassium and high-threshold (L-type) calcium channels were recorded in voltage-clamp mode using the Axon's pClamp 8 program with standard protocols (Figure 1B, C). The data were saved in ASCII format and imported into the MATLAB program. A graphical interface was created to fit the mathematical model to the experimental data and to visualize the results. To quantify the difference between the fitted curves and the recorded data the following error-functions were implemented:

1. Maximum error: $E_{Max} = Max(Abs(R(t_n)-S(t_n)))$ where $R(t_n)$ is the recorded value and $S(t_n)$ is the simulated data at time t_n.
2. Least Square: $E_{Lsquare} = \sum_n((R(t_n)-S(t_n))^2)$.
3. Weighted Least Square: $E_{WLsquare} = E_{Lsquare}$ if $t_n<30$ ms and $E_{WLsquare} = 5 * E_{Lsquare}$ if $t_n \geq 30$ ms.

After several trials it was concluded that simulations using the Weighted Least Square Error function gave the most satisfactory results because the other Error Functions occasionally obtained a non-inactivating sodium-current component in the simulated data. Curves were fitted after an initial 0.1ms delay to eliminate the effect of experimental artifacts. In some simulations the reversal potential for the ionic conductances was kept constant.

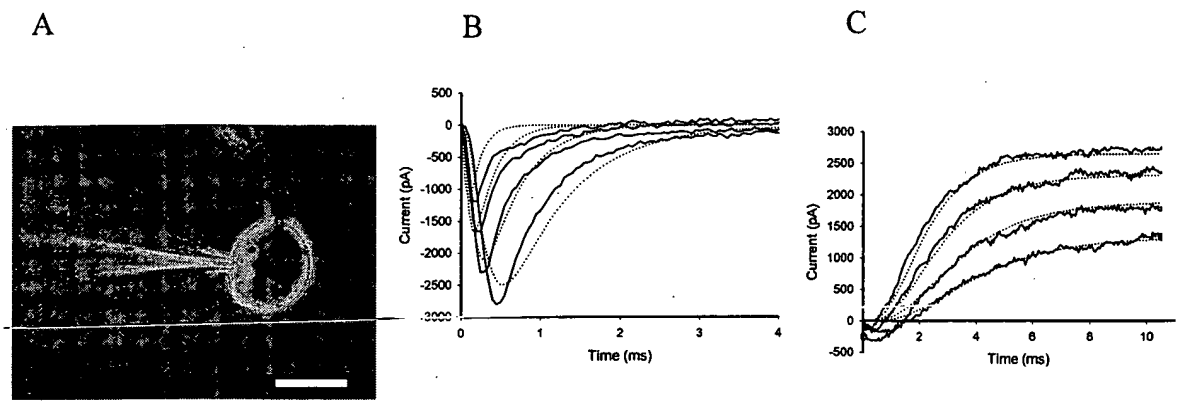

Figure 1. Estimation of ion channel parameters from the voltage-clamp experiments. A: Phase-contrast picture of an NG108-15 cell with a patch-clamp electrode attached to the cell (40x objective, scale bar = 25 μm). B: Sodium currents recorded at different membrane potentials of -10, 0, 10, 20 mV in voltage-clamp mode (solid line) and the results of the parameter fitting using the Hodgkin-Huxley model and the linear thermodynamic formalism (dotted line). C: Potassium currents recorded at membrane potentials of 0, 10, 20 and 30 mV (solid line) and the fitted curves using the model (dotted line).

In general, an excellent fit to the potassium channel data (Figure 1B, C) and an acceptable fit to the sodium and calcium channel data was acheived. The automatic fitting algorithm converged in less than 2 min. running on a Pentium III 1GHz personal computer. After averaging the results of 3-10 experiments the initial parameter values for modeling the action potentials were obtained (Table 1).

					Activation								Inactivation							
Channel	g	SEM	V_{Rev}	SEM	z	SEM	$V_{1/2}$	SEM	ξ	SEM	A	SEM	z	SEM	$V_{1/2}$	SEM	ξ	SEM	A	SEM
Sodium	343.59	183.23	72.35	6.31	5.98	0.30	-46.93	2.46	-0.38	0.01	0.58	0.12	-7.48	1.13	-64.36	4.73	0.41	0.01	1.31	0.17
Potassium	25.09	4.81	-80.00	0.00	2.78	0.46	-22.52	2.64	-0.26	0.02	2.12	0.16								
Calcium	7.45	1.88	32.00	0.00	3.15	0.96	-4.67	6.25	-0.30	0.37	0.84	0.37								
Leakage	5.22	0.89	-49.40	0.76																

Table 1. Average ion channel parameters characteristic of NG108-15 cells obtained by parameter fitting to voltage-clamp data (n = 3-10).

Action potential shape analysis

Action potentials were evoked with short (2 ms) current injections in current clamp mode either at resting membrane potential or at a – 85 mV holding potential. The following parameters were obtained from the patch-clamp recordings and used in the modeling: membrane resistance, resting membrane potential, membrane capacitance and injected current. The maximum conductance of the leakage current (g_l) was calculated from the ionic conductances and from the resting membrane potential. We used the earlier established, averaged ion-channel parameters as the initial parameters for the action potential fitting. Using voltage dependent sodium, potassium and L-type calcium conductances, an excellent fit to the rising and to the initial falling phase of the action potentials in the NG108-15 cells was obtained (Figure 2).

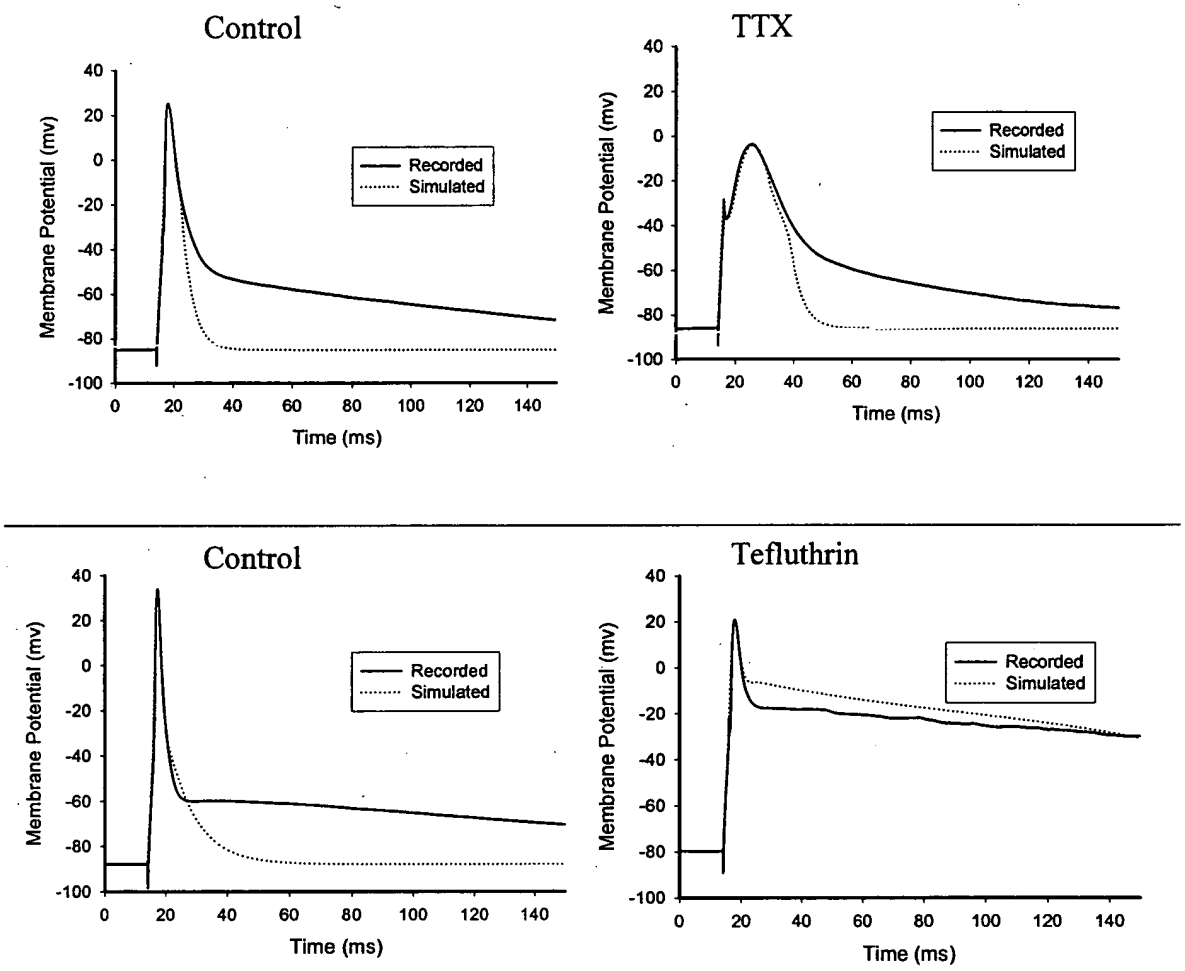

Figure 2. Effect of toxins on the action potentials of NG108-15 cells. Upper panel: effect of 0.5 μM tetrodotoxin. Lower panel: effect of 0.5 μM tefluthrin. Solid line: data recorded in current clamp experiments. Dotted line: results of the simulation using the mathematical model of the NG108-15 cells.

We also obtained an excellent fit to the experimental data in the case of the toxin-modified action potentials by modifying only the corresponding sodium-channel parameters (Figure 2, Table 2).

			Activation				Inactivation			
Na	g	V_{Rev}	z	$V_{1/2}$	ξ	A	z	$V_{1/2}$	ξ	A
Contr	317±84	60	6±0.04	-6.9±0.3	-0.38±0.03	0.59±0.08	-7.5±0.04	-64±0.4	0.43±0.03	1.5±0.7
TTX	31±18	60	6±0.01	-6.9±0.3	-0.40±0.03	0.83±0.17	-7.5±0.1	-64±0.4	0.42±0.02	3.0±0.9
% Chg	**-89±6**	0	-0.6±0.6	0±0.004	5.9±5.2	**41±25.5**	0±0.002	0±0.001	-0.68±0.7	331±301
Contr	227±106	60	5.6±0.4	-46.7±0.2	-0.38±0	0.7±0.12	-7.4±0.1	-60±2.6	0.48±0.01	1.3±0.22
Tefl	44.6±11	60	5.6±0.4	-54±2.3	-0.36±0.02	1.5±0.6	-7.8±0.3	-69±2.1	0.47±0.04	39±18
% Chg	**-71±9**	0	1±1	**17±5**	-4±4.2	86±66	6±5.71	**15±2.2**	-2±7.9	**4410±2974**

Table 2. Effect of TTX and tefluthrin on the action potential parameters. Only sodium channel parameters are shown, the other ion-channel parameters did not change. Data shown as mean ± SEM. Bold: statistically significant ($p > 0.05$) change.

Discussion

We have developed a mathematical model of the action potential generation in NG108-15 cells and extracted the parameters for this model from whole-cell patch clamp experiments. Utilizing only voltage-sensitive sodium, potassium and L-type calcium channels we were able to obtain an excellent fit to the rising as well as to the initial falling phase of the action potential. A linear thermodynamic formalism was used to describe the voltage and time dependence of the ionic conductances, which eliminated the need for 'guessing' the function for the voltage-dependence of the rate constants and the same form (with different parameters) could be used for the characterization of all the ion channels. In order to validate the action potential shape analysis for utilization as a toxin detection method, the effect of two toxins, tetrodotoxin, a specific sodium channel blocker, and tefluthrin, a sodium channel opener pyrethroid were analyzed. Changes in the action potential shape, and also in the fitted ion-channel parameters caused by the two toxins, were measured. An excellent fit to the toxin-modified action potential shapes by modifying only the appropriate sodium channel parameters has been achieved. TTX, as

expected from a channel blocker, significantly decreased the maximum sodium conductance, but did not affect the voltage dependence of the channel (Table 2.). Unexpectedly, TTX effected the activation kinetics of the sodium channels as well. TTX moderately increased the activation **A** parameter by causing a slowing down of the activation of the channel. This effect could be an experimental artifact, because Franceschetti, Lavazza et al. (2003) explained the effect of TTX on the kinetics of the sodium channels with a non-perfect space clamp. Another explanation could be the existence of different subpopulations of sodium channels on the NG108-15 cells with different activation and inactivation time constants and different TTX sensitivities.

The major effect of tefluthrin (a channel opener) was to slow down (practically remove) the inactivation of the sodium channels. Tefluthrin also affected the maximum sodium channel conductance and the voltage dependence of the activation and inactivation of the channel, shifting appropriate current-voltage (I/V) relationships to the left by about 15 mV. A Similar effect on the voltage dependence of the sodium channels was described by Spencer et al. (2001) for fenpropathrin, a tefluthrin-like pyrethroid.

In summary, these experiments indicated that we were able to decipher and quantify the effects of toxins on ion channels without actually measuring ion channel currents in voltage-clamp experiments. Instead, changes in the shape of action potentials measured by patch clamp electrophysiology, combined with a validated computer simulation of the cell, were utilized.

This method could be useful for toxin detection and for classification of unknown toxins in environmental protection scenarios or in the detection of biological and chemical warfare agents. It could also be extended to functional screening in drug

development. With the refinement of the model of the cell not only those toxins could be identified, which are directly acting on ion channels, but also changes in second messenger levels or gene expression could also be detected and classified. Moreover, recent advancements in the study of the cell electrode interface and microelectrode-fabrication technology indicate that high-fidelity extracellular recording of action potential shapes might be possible, which opens a new horizon for the high-throughput application of our method using extracellular recordings.

Acknowledgement

The Hunter endowment at Clemson University and DOE grant number DE-FG02-00ER45856 for funding the study; Dr. M. W. Nirenberg (NIH) for kindly supplying the NG108-15 cell line. Initial experiments were done at Clemson University as indicated by the dual affiliations of Drs. Molnar and Hickman.

References

Agin, D. (1972). Excitability phenomena in membranes. Foundations of Mathematical Biology. R. Rosen. New York, Academic Press: 253-277.

Ahmed, I. A., P. M. Hopkins, et al. (1993). "Caffeine and Ryanodine Differentially Modify a Calcium- Dependent Component of Soma Action-Potentials in Identified Molluscan (Lymnaea-Stagnalis) Neurons in-Situ." Comparative Biochemistry and Physiology C-Pharmacology Toxicology & Endocrinology **105**(3): 363-372.

Akay, M., E. Mazza, et al. (1998). "Non-linear dynamic analysis of hypoxia-induced changes in action potential shape in neurons cultured from the rostral ventrolateral medulla (RVLM)." Faseb Journal **12**(4): 2881.

Amigo, J. M., J. Szczepanski, et al. (2003). "On the number of states of the neuronal sources." Biosystems **68**(1): 57-66.

Baeumner, A. J. (2003). "Biosensors for environmental pollutants and food contaminants." Analytical and Bioanalytical Chemistry **377**(3): 434-445.

Bentleya, A., A. Atkinsona, et al. (2001). "Whole cell biosensors — electrochemical and optical approaches to ecotoxicity testing." Toxicology *in Vitro* **15**: 469-475.

Bousse, L. (1996). "Whole cell biosensors." Sensors and Actuators B-Chemical **34**(1-3): 270-275.

Chiappalone, M., A. Vato, et al. (2003). "Networks of neurons coupled to microelectrode arrays: a neuronal sensory system for pharmacological applications." Biosensors and Bioelectronics **18**: 627-634.

Clark, R. B., R. A. Bouchard, et al. (1993). "Heterogeneity of Action-Potential Wave-Forms and Potassium Currents in Rat Ventricle." Cardiovascular Research **27**(10): 1795-1799.

Cohen, H. (1976). Mathematical developments in Hodgkin-Huxley theory and its approximations. Proceedings of the Ninth Symposium on Mathematical Biology held in New York, January, 1975. S. A. Levin. Washington, The American Mathematical Society: 89-124.

Croston, G. E. (2002). "Functional cell-based uHTS in chemical genomic drug discovery." Trends in Biotechnology **20**(3): 110-115.

Denyer, M. C. T., M. Riehle, et al. (1998). "Preliminary study on the suitability of a pharmacological bio- assay based on cardiac myocytes cultured over microfabricated microelectrode arrays." Medical & Biological Engineering & Computing **36**(5): 638-644.

Destexhe, A. and J. R. Huguenard (2000). "Nonlinear Thermodynamic Models of Voltage-Dependent Currents." Journal of Computational Neuroscience **9**: 259-270.

Djouhri, L. and S. N. Lawson (1999). "Changes in somatic action potential shape in guinea-pig nociceptive primary afferent neurones during inflammation *in vivo*." Journal of Physiology-London **520**(2): 565-576.

Doebler, J. A. (2000). "Effects of neutral ionophores on membrane electrical characteristics of NG108-15 cells." Toxicology Letters **114**(1-3): 27-38.

Dokos, S. C., B. Lovell,N. (1996). "Ion Currents Underlying Sinoatrial Node Pacemaker Activity: A New Single Cell Mathematical Model." Journal of Theoretical Biology **181**(3): 245-272.

Evans, G. P., M. G. Briers, et al. (1986). "Can Biosensors Help to Protect Drinking-Water." Biosensors **2**(5): 287-300.

Franceschetti, S., T. Lavazza, et al. (2003). "Na(+)-activated K+channels and volatge-evoked ionic currents in brain stem and parasympathetic neurones of the chick." Journal of Neurophysiology **89**(4): 2101-2111.

Gross, G. W., A. Harsch, et al. (1997). "Odor, drug and toxin analysis with neuronal networks *in vitro*: Extracellular array recording of network responses." Biosensors & Bioelectronics **12**(5): 373-393.

Gross, G. W., B. K. Rhoades, et al. (1995). "The Use of Neuronal Networks on Multielectrode Arrays as Biosensors." Biosensors & Bioelectronics **10**(6-7): 553-567.

Heck, D. E., A. Roy, et al. (2001). "Nucleic acid microarray technology for toxicology: Promise and practicalities." Biological Reactive Intermediates Vi **500**: 709-714.

Higashida, H., R. A. Streaty, et al. (1986). "Bradykinin-Activated Transmembrane Signals Are Coupled Via No or Ni to Production of Inositol 1,4,5-Trisphosphate, a 2nd Messenger in Ng108-15 Neuroblastoma Glioma Hybrid-Cells." Proceedings of the National Academy of Sciences of the United States of America **83**(4): 942-946.

Hodgkin.L.A and Huxley.F.A (1952). "A quantitative description of membrane current and its application to conduction and excitation in nerve." Journal of Physiology **117**: 500-544.

Hu, Q., F. Huang, et al. (1997). "Inhibition of Toosendanin on the delayed rectifier potassium current in neuroblastoma X glioma NG108-15 cells." Brain Research **751**: 47-53.

Jorkasky, D. K. (1998). "What does the clinician want to know from the toxicologist?" Toxicology Letters **102-103**: 539-543.

Jung, D. R., D. S. Cuttino, et al. (1998). "Cell-based sensor microelectrode array characterized by imaging x-ray photoelectron spectroscopy, scanning electron microscopy, impedance measurements, and extracellular recordings." Journal of Vacuum Science & Technology a-Vacuum Surfaces and Films **16**(3): 1183-1188.

Kinter, L. B. and J. P. Valentin (2002). "Safety pharmacology and risk assessment." Fundamental & Clinical Pharmacology **16**(3): 175-182.

Krause, M., S. Ingebrandt, et al. (2000). "Extended gate electrode arrays for extracellular signal recordings." Sensors and Actuators B **70**: 101–107.

Lukyanetz, E. A. (1998). "Diversity and properties of calcium channel types in NG108-15 hybrid cells." Neuroscience **87**(1): 265-274.

Ma, W., G. M. Grant, et al. (1999). "Kir 4.1 channel expression in neuroblastoma×glioma hybrid NG108-15 cell line." Developmental Brain Research **114**(1): 127-134.

Ma, W., J. J. Pancrazio, et al. (1998). "Neuronal and glial epitopes and transmitter-synthesizing enzymes appear in parallel with membrane excitability during neuroblastoma X glioma hybrid differentiation." Developmental Brain Research **106**: 155-163.

Martin-Caraballo, M. and J. J. Greer (2000). "Development of potassium conductances in perinatal rat phrenic motoneurons." Journal of Neurophysiology **83**(6): 3497-3508.

Mason, T. W. (1993). Fluorescent and Luminescent Probes for Biological Activity. London, Academic Press.

Morefield, S. I., E. W. Keefer, et al. (2000). "Drug evaluations using neuronal networks cultured on microelectrode arrays." Biosensors & Bioelectronics **15**(7-8): 383-396.

Muraki, K., Y. Imaizumi, et al. (1994). "Effects of Noradrenaline on Membrane Currents and Action- Potential Shape in Smooth-Muscle Cells from Guinea-Pig Ureter." Journal of Physiology-London **481**(3): 617-627.

Naessens, M. and A. Tran-Minh (1998). "Whole-cell biosensor for determination of volatile organic compounds in the form of aerosols." Analytica Chimica Acta **364**(1-3): 153-158.

Naessens, M. and C. Tran-Minh (1998). "Whole-cell biosensor for direct determination of solvent vapours." Biosensors & Bioelectronics **13**(3-4): 341-346.

Nygren, A., C. Fiset, et al. (1998). "Mathematical model of an adult human atrial cell - The role of K+ currents in repolarization." Circulation Research **82**(1): 63-81.

Offenhausser, A. and W. Knoll (2001). "Cell-transistor hybrid systems and their potential applications." Trends in Biotechnology **19**(2): 62-66.

Ohlstein, E. H., R. R. Ruffolo, et al. (2000). "Drug discovery in the next millennium." Annual Review of Pharmacology and Toxicology **40**: 177-191.

Otten, E. H., M.Scheepstra K,A. (1995). "A model study on the influence of a slowly activating potassium conductance on repetitive firing patterns of muscle spindle primary endings." Journal of Theoretical Biology **173**(1): 67-78.

Paddle, B. M. (1996). "Biosensors for chemical and biological agents of defence interest." Biosensors & Bioelectronics **11**(11): 1079-1113.

Philp, J. C., S. Balmand, et al. (2003). "Whole cell immobilised biosensors for toxicity assessment of a wastewater treatment plant treating phenolics-containing waste." Analytica Chimica Acta **487**: 61–74.

Rogers, K. R. (1995). "Biosensors for Environmental Applications." Biosensors & Bioelectronics **10**(6-7): 533-541.

Schaffner, E. A., L. J. Barker, et al. (1995). "Investigation of the factors necessary for growth of hippocampal neurons in a defined system." Journal of Neuroscience Methods **62**: 111-119.

Schmitt, H. and H. Meves (1995). "Model experiments on squid axons and NG108-15 mouse neuroblastoma * rat glioma hybrid cells." Journal of Physiology (Paris) **89**: 181-193.

Shaw, R. M. and Y. Rudy (1997). "Electrophysiologic effects of acute myocardial ischemia: a theoretical study of altered cell excitability and action potential duration." Cardiovascular Research **35**(2): 256-272.

Shevtsova, N. A. P., K.McCrimmon,D. R.Rybak,I. A. (2003). "Computational modeling of bursting pacemaker neurons in the pre-Bötzinger complex." Neurocomputing **52-54**: 933-942.

Spencer, C. I., K. H. Yuill, et al. (2001). "Actions of Pyrethroid Insecticides on Sodium Currents, Action Potentials, and Contractile Rhytm in Isolated Mammalian Ventricular Myocytes and Perfused Hearts." The Journal of Pharmacology and Experimental Therapeutics **298**: 1067-1082.

Stett, A., U. Egert, et al. (2003). "Biological application of microelectrode arrays in drug discovery and basic research." Analytical and Bioanalytical Chemistry **377**(3): 486-495.

Tojima, T., Y. Yamane, et al. (2000). "Acquisition of neuronal proteins during differentiation of NG108-15 cells." Neuroscience Research **37**: 153-161.

Tzoris, A., D. Fearnside, et al. (2002). "Direct toxicity assessment of wastewater: Baroxymeter, a portable rapid toxicity device and the industry perspective." Environmental Toxicology **17**(3): 284-290.

van Soest, P. F. and K. S. Kits (1998). "Conopressin affects excitability, firing, and action potential shape through stimulation of transient and persistent inward currents in mulluscan neurons." Journal of Neurophysiology **79**(4): 1619-1632.

Weiss, I., A. Urbaszek, et al. (1995). "Simulation of the Cardiac Action-Potentials of Various Cell- Types with Account Being Taken of Neural Influencing Factors." Biomedizinische Technik **40**(3): 64-69.

Weiss, T. F. (1996). Cellular Biophysics. Cambridge, MA, The MIT Press.

Xia, Y., K. V. Gopal, et al. (2003). "Differential acute effects of fluoxetine on frontal and auditory cortex networks *in vitro*." Brain Research **973**(2): 151-160.